Pressure-induced phase-transition of $YBa_2Cu_4O_8$

Atsuko Nakayama[1,*], Yusuke Onda[2], Shuhei Yamada[2], Hiroshi Fujihisa[3],
Satoshi Nakano[4], Ayako Ohmura[1], Fumihiro Ishikawa[5], Yuh Yamada[5]
[1]Center for Transdisciplinary Research, Niigata University, Niigata 950-2181, Japan
[2]Graduate School of Science and Technology, Niigata University, Niigata 950-2181, Japan
[3]Nat'l Institute of Advanced Industrial Science and Technology (AIST), Tsukuba 305-8565, Japan
[4]Nat'l Institute for Materials Science (NIMS), Tsukuba 305-0044, Japan
[5]Department of Physics, Niigata University, Niigata 950-2181, Japan

The crystal structure of $YBa_2Cu_4O_8$ (Y124) was studied under high pressure up to 18 GPa. Y124 causes the first-order phase-transition into the orthorhombic *Immm* at pressure around 11 GPa. The CuO_2 plane persists in the high-pressure phase but the CuO double chains collapse and transform into three-dimensional Cu-O network, resulting in the suppression of superconductivity.

1 Introduction

$YBa_2Cu_4O_8$ (Y124) is one of the high transition temperature (T_c) superconductors with T_c = 80 K at atmospheric pressure [1]. The pressure dependence of T_c linearly increases up to 5 GPa however decreases after passing through the maximum T_c = 108 K at 12 GPa [2]. Continues changes in lattice parameters of Y124 was observed under pressure up to 25 GPa using a diamond anvil cell (DAC) and NaF pressure-transmitting medium (PTM) [3]. The resistance of bulk ceramic of Y124 in magnetic fields up to 10 T showed the parabolic and continuous pressure dependence on T_c [4].

On the other hand, recent research has pointed out the anomaly of pressure-induced structural-change of Y124 under pressures above 3.7 GPa [5]. The synchrotron powder x-ray diffraction (XRD) measurement, using a methanol-ethanol mixture as PTM, revealed that Y124 shows pressure-induced lattice anomalies and hysteresis in the pressure dependence of the lattice parameters in the range from 3.7 to 12 GPa.

The discrepancy between the two reports on structure (Refs. 3 and 5), should be induced by hydrostaticity from PTM. The use of helium (He) as PTM brings quasi-hydrostaticity under pressure over 10 GPa significantly decreases the effect of uni-axial stress, resulting in the sharp diffraction pattern under high pressure [6]. In order to clarify the conduction mechanism of Y124 under high pressure especially above 10 GPa, we carried out powder XRD under pressure up to 18 GPa and at room temperature (RT) under hydrostatic condition using He.

2 Experiment

The polycrystalline Y124 compound for powder XRD measurement was synthesized by a high-oxygen pressure-technique [1]. The sample obtained was ground into fine powders in an alumina mortar cooled in liquid nitrogen.

XRD patterns were measured by using the DAC set up a couple of diamond anvils with 0.6-mm culet-diameters and 2-mm anvil-thicknesses. The gasket was made of 65-μm-thick stainless steel, in which a 260-μm hole was drilled. A small amount of powdered sample was put in the gasket hole mounted on the culet of lower anvil with ruby balls, which was filled with high-density He-gas [7]. Each pressure was determined from the fluorescence peaks of ruby balls put in the sample chamber on the basis of ruby pressure scale [8].

Angle-dispersive powder-patterns were taken using synchrotron radiation from the bending magnet on the beam-line BL-18C at Photon Factory, High Energy Accelerator Research Organization (KEK). The beam was monochromatized to a wavelength 0.6190 Å and introduced to the specimen through a pinhole collimator with 80 μm diameter. Each pattern was obtained by having the sample exposed to the x-ray for 20 min at RT. An imaging plate and a BAS2500 scanner, supplied by Fuji Photo Film Co. Ltd., were used to obtain two-dimensional powder diffraction image.

3 Results and Discussions

The pressurization above 10.1 GPa causes the change in the pattern accompanied with drastic decrease of the 00l reflections (l = 2, 4 and 6). The reflections derived from the Cu-O double-change structure, 104 and 106, disappeared at 11.0 GPa. These are the evidence that the structural-phase transition occurs at around 11 GPa. The XRD pattern of released sample recovered to the original.

The crystal structure of high-pressure phase (HPP) has been determined by Rietveld analysis [9] and molecular dynamic (MD) simulation based on a density-functional theory (DFT). The DFT calculations for structural optimizations and MD simulations were carried out using the program MS CASTEP of Accelrys, Inc [10]. We employed the generalized-gradient approximation (GGA) - Perdew-Burke-Ernzerhof for solids (PBEsol) exchange correlation functional [11] and ultrasoft pseudopotentials [12] with the energy cut-off of 440 eV.

The structure after the phase transition is assigned to be an orthorhombic with the space group *Immm* through Rietveld fit. Wang *et al*. also reported the phase transition to orthorhombic at 11 GPa; they chose non-centrosymmetric orthorhombic the space group *Imm*2 [13]. Both *Immm* and *Imm*2 space groups are explained by a same extinction rule; either is suitable to explain the peak positions observed in the XRD patterns of HPP.
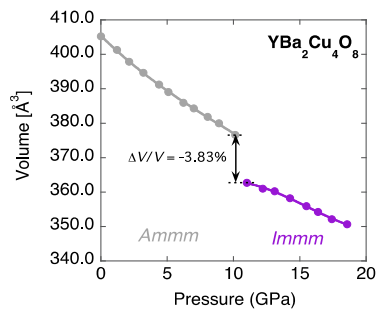
(a)
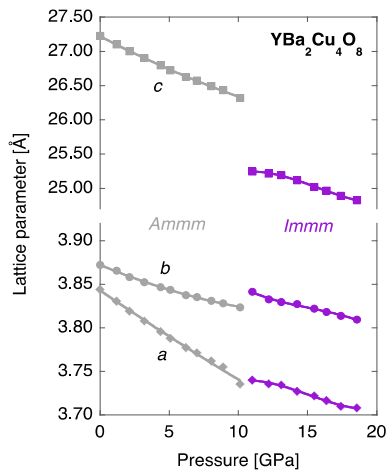
(b)

Fig. 1: Pressure changes in (a) the lattice parameters *a*, *b*, and *c*, and (b) volume *V* of Y124 up to 18.1 GPa at room temperature.

Analyses of internal structures using both space groups, respectively, produced the same structure. Therefore we chose the centrosymmetric space group *Immm* for the crystal structure of HPP.

The pressure changes in lattice parameters *a*, *b*, and *c*, and volume *V,* are shown in Fig. 1(a) and (b), respectively. The *b*-axis length temporary enhances just after the phase transition while decreases with increasing the pressure in HPP. The *c*-axis length at 11.0 GPa is 3.8 % shorter than that at 10.1 GPa. The change in volumes measured before and after the transition is obtained to be V / V = -3.83 %.

Projections on the *ab* plane of crystal structures obtained before and after the phase transition are shown in Fig. 2. The phase transition of Y124 is explained as follows: The unit cell is pulled in opposite directions along the *a* axis, resulting in deformation into the monoclinic in HPP. We were able to replace the monoclinic with the orthorhombic, which is higher in the symmetry than the monoclinic. In this way the crystal structure of HPP was determined to be the *Immm* structure. Every quadrangular pyramid consisting of the apical oxygen atom and CuO_2 basal plane, maintains after phase transition. However the CuO double-chains structure, perpendicular to the *ac* plane, is broken after phase transition and three-dimensional Cu-O network are generated in HPP.

Temperature dependence of electrical resistance dramatically changes in the temperature dependence by pressurization exceeding 9.7 GPa; the vale of T_c drastically decreases at above 9.7 GPa [14]. That is clearly different from the previous result [4]. Assuming
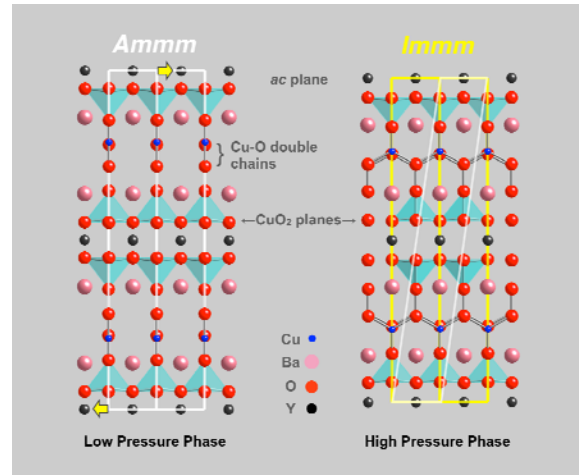
that the pressure-induced structural-phase transition also occurs at around 11 GPa at low temperature, the negative pressure dependence of T_c is an essential feature for HPP. It is believed that the depression of T_c observed above 9.7 GPa is caused by collapse of the CuO double chains to supply the carriers. On the other hand the CuO_2 plane persists in HPP. This means that the CuO_2 plane plays the role of conductive layer in both LPP and HPP. After the dramatic decrease of T_c a distribution of conduction electrons on the CuO_2 plane seems to change after the phase transition.

4 Summary

XRD of $YBa_2Cu_4O_8$ shows the presence of pressure-induced phase-transition at pressure around 11 GPa. The CuO_2 plane persists in HPP, having the orthorhombic *Immm*. The CuO_2 plane plays the role of conductive layer in both LPP and HPP. On the other hand the CuO double chains collapse after phase transition, resulting in another Cu-O bonding structure. Decreasing of T_c with increasing the pressure is caused by the collapse of CuO double chains.

References
[1] J. Karpinski, E. Kaldis, E. Jilek, S. Rusiecki, B. Bucher, *Nature* **336**, 660 (1988).
[2] E. N. Van Eenige, R. Griessen, and R. J. Wijngaarden, *Physica C* **168**, 482 (1990).
[3] H. A. Ludwig, W. H. Fietz, M. R. Dietrich, H. Wühl, J. Karpinski, E. Kaldis, and S. Rusiecki, *Physica C* **167**, 335 (1990).
[4] J. J. Scholtz, E. N. van Eenige, R. J. Wijngaarden, and R. Griessen, *Phys. Rev. B* **45**, 3077 (1992).
[5] M. Calamiotou, A. Gantis, E. Siranidi, D. Lampakis, J. Karpinski, E. Liarokapis, *Phys. Rev. B* **80**, 214517 (2009).
[6] K. Takemura, *Phys. Rev. B* **60**, 6171 (1999).
[7] K. Takemura, P. Ch, Sahu, Y. Kunii, and Y. Toma, *Rev, Sci. Instrum*. **72**, 3873 (2001).

[8] C. S. Zha, H. K. Mao, and R J. Hemlsy, *Proc. Natl., Acad. Sci.,* **97**, 13494 (2000).

[9] F. Izumi, in *The Rietveld Analysis*, ed. R. A. Young, (Oxford University Press, New York, 1993) p. 236.

[10] S. J. Clark, M. D. Segall, C. J. Pickard, P. J. Hasnip, M. I. J. Probert, K. Refson, and M. C. Payne, *Z. Kristallogr.* **220**, 567 (2005).

[11] J. P. Perdew, A. Ruzsinszky, G. I. Csonka, O. A. Vydrov, G. E. Scuseria, L. A. Constantin, X. Zhou, and K. Burke, *Phys. Rev. Lett.* **100**, 136406 (2008).

[12] D. Vanderbilt, *Phys. Rev. B* **41**, 7892 (1990).

[13] X. Wang, F. H. Su, S. Karmakar, K. Syassen, Y. T. Song and C. T. Lin, in *Max-Planck-Institut für Festkörperforschung Stuttgart Annual Rep.*, 70 (2007).

[14] A. Nakayama, Y. Onda, S. Yamada, H. Fujihisa, M. Sakata, Y. Nakamoto, K. Shimizu, S. Nakano, A. Ohmura, F. Ishikawa and Y. Yamada, *J. Phys. Soc. Jpn.*, **83**, 093601 (2014).

* nakayama-a@phys.sc.niigata-u.ac.jp